Scientia Iranica A (2017) 24(2), 537–550

Sharif University of Technology
Scientia Iranica
Transactions A: Civil Engineering
www.scientiairanica.com

Stability of supported vertical cuts in granular matters in presence of the seepage flow by a semi-analytical approach

M. Veiskarami[a,b,*] and S. Fadaie[b]

a. *School of Engineering, Shiraz University, Shiraz, Iran.*
b. *Faculty of Engineering, University of Guilan, Rasht, Iran.*

Received 31 October 2015; received in revised form 1 December 2015; accepted 18 June 2016

KEYWORDS
Stability;
Complex analysis;
Stress characteristics;
Seepage;
Granular matter.

Abstract. Vertical cuts are prone to several types of failure such as piping, ground heaving, and deep-seated or base failure. The latter is the subject of this study and probably attracts less attention in comparison to other types of failure. Although it is commonly believed that such a failure is rare in normal conditions; in presence of the seepage flow, deep-seated failure is much likely to initiate and advance prior to other types of failure. In this paper, the stability analysis of vertical cuts in granular soils in presence of the seepage flow is studied against the deep failure. To do so, the stability analysis is made by the use of the well-known method of stress characteristics with inclusion of the seepage flow force. This nonuniform flow field renders the stability analysis quite complex. A semi-analytical approach, based on complex algebra, is presented to find the flow field, which is accurate and much faster for calculation of the seepage force at arbitrary points in the field. The solution of the flow field is a background solution for the stress field which is to be found to assess the stability.

1. Introduction

Stability problems in soil mechanics may be stemmed from historical contributions of Coulomb (1776) and Rankine (1857) including the slope stability, bearing capacity, and lateral earth pressure problems as classical problems [1,2]. For stability analysis of vertical cuts, some of such problems are involved and should be checked. In this regard, according to Terzaghi (1943), two major types of failure of vertical cuts are the slope failure and the base (or deep-seated) failure [3]. As vertical cuts in granular soils are often supported by either flexible or rigid retaining structures, the first kind of failure, i.e. the slope failure, is seldom a problem; instead, conventional approaches are focused on the estimation of the lateral earth pressure and/or stability against the deep-seated failure. In many cases, vertical cuts are excavated below the groundwater table or adjacent to rivers or banks. As a result, there will be another type of failure beside the slope or the base failure, which is attributed to the piping or ground heaving due to the seepage flow.

The literature review behind the stability analysis for problems addressed above is rather long and rich with contributions including the force limit equilibrium methods (classically Coulomb, 1776; more recently Kumar and Subba Rao, 1997; Subba Rao and Choudhury, 2005; Barros, 2006; Ghosh, 2008; Ghosh and Sharma, 2012; Barros and Santos, 2012; Ling et al., 2014) [1,4-

*. *Corresponding author. Tel.: +98 71 36133102; Fax: +98 71 36473161*
E-mail addresses: mveiskarami@shirazu.ac.ir (M. Veiskarami); sinafadaie@gmail.com (S. Fadaie)

10], method of stress characteristics (Sokolovskii, 1965; Larkin, 1968; Sabzevari and Ghahramani, 1972 and 1973; Houlsby and Wroth, 1982; Kumar, 2001; Kumar and Chitikela, 2002) [11-17] or the limit analysis (Chen, 1969; Lysmer, 1970; Chen and Davidson, 1973; Collins, 1973; Chen, 1975; Arai and Jinki, 1990; Soubra, 2000; Soubra and Macuh, 2002; Shiau et al., 2008; Jahanandish et al., 2010; Veiskarami et al., 2014) [18-28], among others. Attempts to include the effect of the groundwater flow in the stability analysis may date back to Terzaghi (1943) who studied the stability of the soil mass in the vicinity of sheet pile walls [3]. Many similar problems have been studied so far which include the effect of the groundwater flow on the bearing capacity and the earth pressure on retaining walls [9,29-31]. In 1999, Soubra and his coworkers studied the important problem of the passive earth pressure on sheet pile walls subjected to the seepage flow and associated hydraulic gradients [32]. In this regard, Barros (2006) [6], Benmebarek et al. (2006) [33], Barros and Santos (2012) [9] and most lately, Santos and Barros (2015) [34] investigated active and passive earth pressures problems in presence of the seepage. Recently, Veiskarami and Zanj (2014) made an attempt to include the seepage force in the stress characteristics equations and compute the passive earth pressure on sheet pile walls subjected to the groundwater flow [35]. They employed the finite element technique to solve the flow field as a background solution which is assumed to remain uninfluenced by the stress field at the limiting equilibrium. The background finite element mesh was then used to interpolate the seepage force through the stress field at the limiting equilibrium.

Although evidence indicated that both the bearing capacity and earth pressure problems in presence of the seepage flow are investigated by researchers, no attempt is known to the authors dealing with the particular problem of the deep-seated failure adjacent to the supported vertical cuts. In this research, this is the matter of focus. The stability analysis involves complexities due to the complex form of the seepage flow behind vertical cuts. The general methodology to investigate this problem is based on the assumptions made by Veiskarami and Zanj (2014) [35] who formally assumed that the seepage flow field is only a function of the geometry of the problem domain and does not change with the formation of the failure mechanism at the limiting state. Therefore, the solution of the flow field can be found independent of the solution of the stress field. Moreover, an analytical solution of the flow field will be presented which obviates any further need for numerical solutions like that of Veiskarami and Zanj (2014) [35]. What comes next comprises the statement of the problem, field equations, and solution techniques.

2. Statement of the problem

A vertical cut in a granular matter cannot be advanced without a lateral support. Such supports are often provided with flexible walls with a series of struts and wales as a bracing system, internal ground anchor supports, mechanically stabilized soil system with facing elements, facing elements, and external supports or other systems [36,37]. Figure 1 shows a number of techniques which can be applied to low-depth and deep excavations. For excavations where the height of the wall is small, a cantilever sheet pile can be used with additional depth extended into the ground to provide the required flexural stiffness which is schematically depicted in Figure 1(a). Such walls can be enhanced with ground anchor (Figure 1(b)) to increase their stiffness and reduce their deflection and lateral displacement. For deep excavations, sheet pile walls must be internally or externally supported as illustrated in Figure 1(c) and (d). In staged construction, as the excavation advances into the ground, facing elements, often consisting of a welded wire mesh faced with shotcrete, steel sheets, etc., are installed at each stage. The wall (facing) is sequentially supported by external or internal support system. This is schematically shown in Figure 1(e) and (f). Unlike the cantilever retaining walls, in many cases, the wall is not extended into the ground in other soil supporting and wall construction techniques, or the extension length can be ignored in comparison to the wall height or due to its flexibility. Therefore, it will be of particular importance to analyze the stability of such systems against a deep-seated (bearing capacity) failure, especially when the seepage flow exists towards the bottom of the cut.

Figure 1(g) schematically represents the simplified problem (a braced or supported excavation in the vicinity of a bank or a river) which coincides with most cases where the excavation is performed with sheet pile walls or facing elements. In this problem, the existence of the seepage flow should be paid special attention. The seepage flow towards the bottom of the cut is a serious problem as it causes the increase in the lateral earth pressure on the supporting system and may lead to piping or heaving failures. In addition, the deep-seated or the bearing capacity failure becomes a serious problem as the seepage force not only multiplies the actuating downward forces, but it also reduces the mobilized strength in the passive zone beneath the bottom of the cut.

Figure 1(h) illustrates the statement of the problem which is investigated theoretically. In this figure, the formation of a failure mechanism in terms of a deep-seated (or bearing capacity) problem is presented within a shaded area BCDQ. This area contains a mass of soil, which is assumed to be at plastic limiting

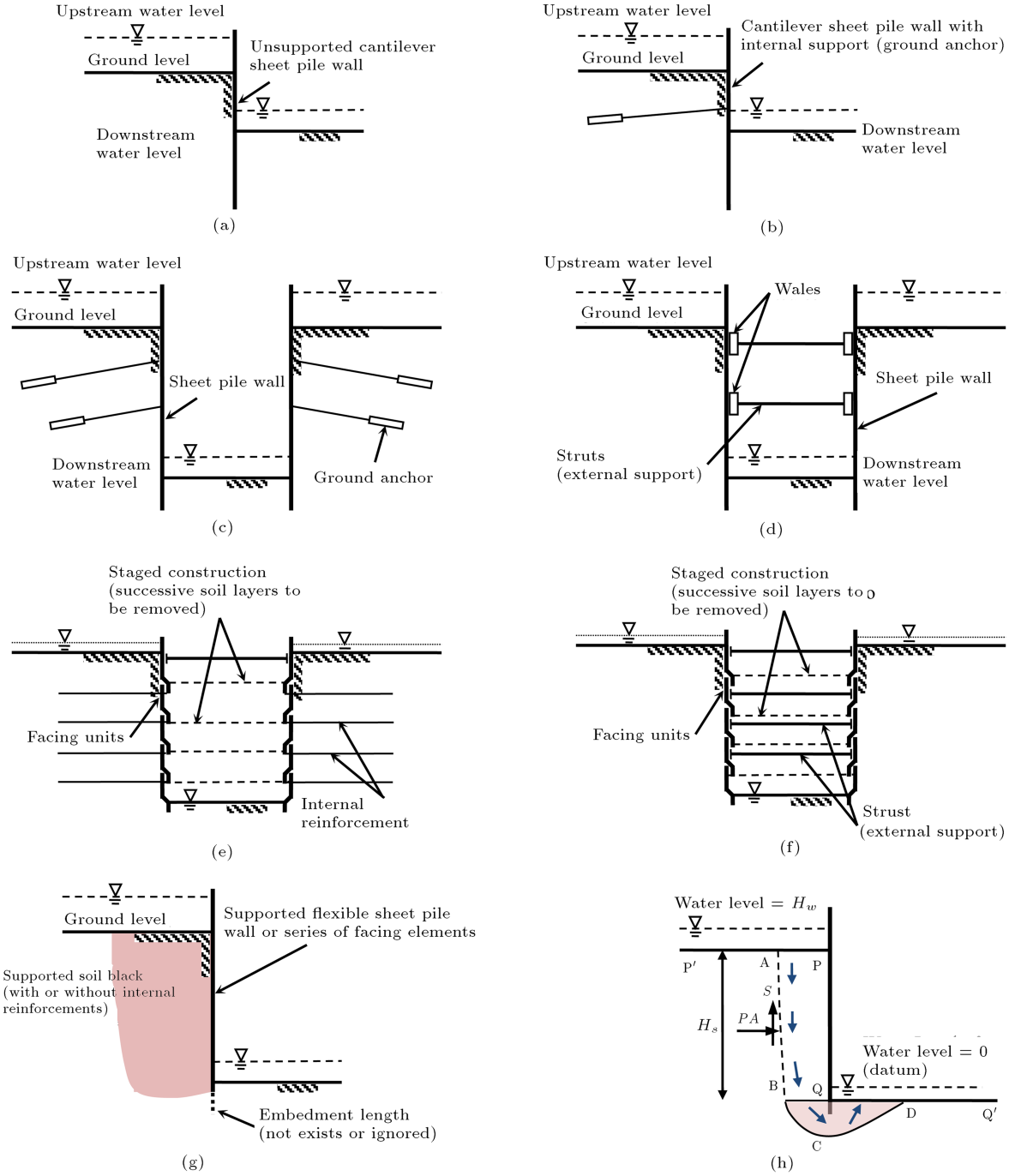

Figure 1. Supported excavations in granular soil: (a) Low-depth excavation with cantilever sheet pile wall, (b) low-depth excavation with cantilever sheet pile wall and internal support, (c) deep excavation with internal supports (ground anchor) and flexible sheet pile wall, (d) deep excavation with external support system (struts), (e) deep excavation with facing units, internally reinforced soil and staged construction, (f) deep excavation with facing units, external support system, and staged construction, (g) simplified and idealized problem, and (h) statement of the solved problem.

equilibrium. The seepage force with a downward direction behind the wall increases the unbalancing force in ABQP soil block. On the other hand, it is evident that the seepage flow in the plastic region causes a reduction in the resistance against deep-seated failure. Therefore, the problem that should be analyzed is similar to a bearing capacity problem involving a seepage force field, for which there is no simple solution.

To analyze this problem, one should determine the ability of soil to withstand the unbalancing force which is received from both the submerged weight of the soil in ABQP region intensified by a downward seepage flow force. Moreover, the existence of the

seepage flow in the plastic region causes a rather complex problem which is required to be solved to find a factor of safety. In this regard, according to Terzaghi (1943) [3], the failure is caused by the weight of the soil block within ABQP region. In addition to the shear resistance within the plastic region BCDQ, some lateral shear resistance is mobilized along the nearly vertical side AB (which is proportional to lateral earth pressure, P_A). One should note that the flexible nature of the wall and its lateral deflections permit mobilization of any significant shear resistance at the interface of the soil block ABQP and the equivalent footing BQ at its base. This is also stated by Terzaghi (1943) [3]. Moreover, the lateral earth pressure can be assumed to obey the active condition. Therefore, the global factor of safety against deep-seated failure, as also expressed by Terzaghi (1943) [3], can be defined as follows:

$$F_S = \frac{\text{Sum of resisting forces}}{\text{Sum of driving forces}} = \frac{Q_{\text{ult}}}{W'_{\text{ABQP}} + F_{fd} - S}, \quad (1)$$

where F_s is the factor of safety against deep-seated failure, W'_{ABQB} is the submerged weight of soil block, ABQP, F_{fd} is the downward seepage flow force through the soil block ABQP, S is the lateral shear resistance acting along boundary AB, and Q_{ult} is the capacity of the equivalent footing BQ at the bottom of the soil block, ABQP. The ultimate pressure tolerable by the soil mass can be reasonably computed by conventional bearing capacity equation for a surface footing on a granular material as follows:

$$Q_{\text{ult}} = f_\gamma \gamma' B'^2 N_\gamma. \quad (2)$$

In this equation, γ' is the submerged unit weight of the soil, B' is the width of the equivalent footing (BQ, yet unknown), N_γ is the third bearing capacity factor which includes the effect of weight, and f_γ is a correction factor which accounts for the effect of the seepage flow and is equal to unity when the seepage flow does not exist. This correction factor has been presented by Kumar and Chakraborty (2012) [30] or Veiskarami and Habibagahi (2013) [38] for a horizontal seepage flow or by Veiskarami and Kumar (2013) [31] for inclined flow. However, for this very complex form of the seepage flow, there is no such factor available. Fortunately, a particular procedure may involve direct solution to the problem described above without requiring the bearing capacity factor, N_γ, and the correction factor, f_γ, to be computed separately. In the procedure presented in this research, the ultimate resistance, Q_{ult}, is computed directly which automatically contains the effect of the seepage flow force. In essence, the factor of safety, F_s, will be the direct outcome of this research which involves all necessary and still undefined parameters like the pattern and intensity of the seepage flow, the width of the equivalent footing, B', and so on.

As stated earlier, one should notice that in spite of possible extension of the sheet pile deeper into the ground, deep-seated failure would still be possible as such a flexible wall may not be able to properly provide a lateral stiffness and/or sufficient embedment depth against the plastically deforming mass. Therefore, the case under study can be regarded as the critical case which can be applied to cases with or without extension of the sheet pile into the ground. Therefore, as the most critical case, such an extended depth (if it probably exists) is ignored.

3. Solution of the flow field

The statement of the flow problem can be easily understood with regard to Figure 1. This is mathematically equivalent to a mixed Dirichlet-Neumann type problem where either the potential head or the flux is prescribed along different boundaries. For instance, the bedrock or any impervious layer is assumed to be reasonably deep into the soil. Thus, the statement of the problem can be mathematically expressed as a flow problem through a "degenerated" semi-infinite domain consisting of three different boundaries: (i) along the boundary P′P, i.e. from minus infinity to the top of the wall, the potential head or the water head is prescribed, i.e., it is equal to H_w, and hence, this is a Dirichlet-type boundary condition; (ii) along the boundary PQ, i.e. along the wall, there is no flux which is equivalent to a Neumann-type boundary condition; (iii) along the boundary QQ′, i.e. from the bottom of the cut to the plus infinity, the water head is zero (datum) and again, a Dirichlet boundary condition exists. The steady-state flow equation can be expressed as follows:

$$\nabla^2 h = 0, \quad (3)$$

where $h = h(x, y)$ is the water head at arbitrary point within the problem domain as the main field variable and ∇^2 (or equivalently $\boldsymbol{\nabla}.\boldsymbol{\nabla}$) is the Laplacian operator.

For this problem, different solutions exist [34,39-43]. Basic elements for the analytical solution can be separately found in text books on complex analysis and also in Harr (1962) [39]. Here, we present only the important details.

The ingredients of computational procedures are to find a solution to the Laplace equation (governing equation to the steady state flow) for a simple domain with a known solution in terms of a complex function, and then transforming the domain, the solution and the gradient of the solution into the domain of interest (main problem domain). To show the procedure, the steady-state flow problem in a semi-infinite plane with Dirichlet and Neumann boundary conditions is prescribed along the boundaries, as shown in Figure 2(a). Note that the problem is defined in the complex plane.

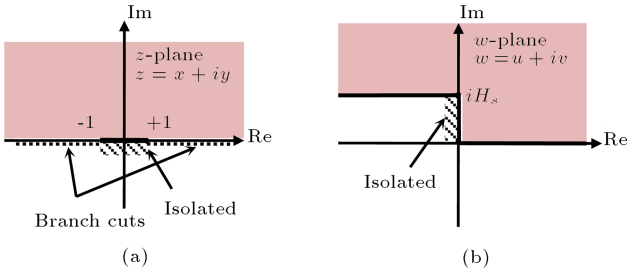

Figure 2. Problem domains: (a) Upper half-plane and (b) main problem domain (transformed).

The boundary conditions are comprised of a constant unit hydraulic head distributed along the semi-infinite line from $-\infty$ to -1 (Dirichlet type); isolated line segment from -1 to +1 (Neumann type); and a constant zero hydraulic head from +1 to $+\infty$ (Dirichlet type). Therefore, the solution function, $h(z) = h(x, y)$, can be mathematically expressed as follows:

$$\nabla^2 h = 0. \tag{4a}$$

Subject to:

$$\begin{cases} h = 1 & \text{from } -\infty \text{ to } -1 \\ h = 0 & \text{from } +1 \text{ to } +\infty \\ \boldsymbol{\nabla} h.\mathbf{e_y} = \frac{\partial h}{\partial y} = 0 & \text{from } -1 \text{ to } +1 \end{cases} \tag{4b}$$

where $\mathbf{e_y}$ is the unit base vector along the y-axis or normal to the x-axis.

This is now necessary to find the solution in the upper half plane, and then transform it to the main problem domain shown in Figure 2(b). To handle this problem and others like this, it is convenient to employ the conformal mapping technique of the complex algebra. A mapping in complex plane, $w = f(z)$, is said to be conformal at some arbitrary point, z_c, if it is both analytic and its derivative is nonzero at that point:

$$f'(z_c) \neq 0. \tag{5}$$

One important property of conformal mapping is that it transforms orthogonal curves into orthogonal curves. This is useful when the steady-state seepage flow is studied. Another important property of such transformations is their ability in the transformation of functions satisfying the Laplace equation. Such functions are real valued functions of $z = x + iy$ and known as harmonic functions which possess continuously the first and second partial derivatives and satisfy the Laplace equation. An important theorem in complex analysis states that if an analytic function ($f(z)$) transforms some domain (D_z) in the z-plane onto another one (D_w) in the w-plane, then if a function $h_w(w) = h_w(u, v)$ is harmonic in D_w, the function $h_D(z) = h_D(x, y) = h_w(u(x, y), v(x, y))$ will be also harmonic in D_z [44]. This enables the application of conformal mapping in solution of Laplace equation in all domains obtained by conformal mapping. To further advance this problem, the solution to the Laplace equation in the upper half-plane is sought first, and then it will be extended to the domain of interest. To do so, consider the semi-infinite strip in w_3-plane, shown in Figure 3(a), with its base isolated and its sides involving Dirichlet boundary conditions as follows:

$$\begin{cases} h = 1 & \text{from } 0 \text{ to } +i\infty \\ h = 0 & \text{from } \pi/2 \text{ to } 1 + i\infty \\ \boldsymbol{\nabla} h.\mathbf{e_{v_3}} = \frac{\partial h}{\partial v_3} = 0 & \text{from } 0 \text{ to } \pi/2 \end{cases} \tag{6}$$

where $w_3 = u_3 + iv_3$, and $\mathbf{e_{(v_3)}}$ is the unit base vector normal to u_3-axis and $h = h(w_3)$. The complete solution to this problem, e.g. by inspection, can be simply expressed as the following unique closed-form solution satisfying both the equation and boundary conditions in w_3-plane:

$$h(u_3, v_3) = 1 - \frac{2}{\pi} u_3, \tag{7}$$

Now, a series of successive transformations will provide the solution in the upper half-plane of the complex plane, i.e. in z-plane. With reference to Figure 3(a) through (d), these transformations will eventually lead to the transformation of both the geometry and the solution onto the complex z-plane.

Appendix A represents all successive transformations with details found in texts on complex analysis [44,45]. Note that in all these equations w_k =

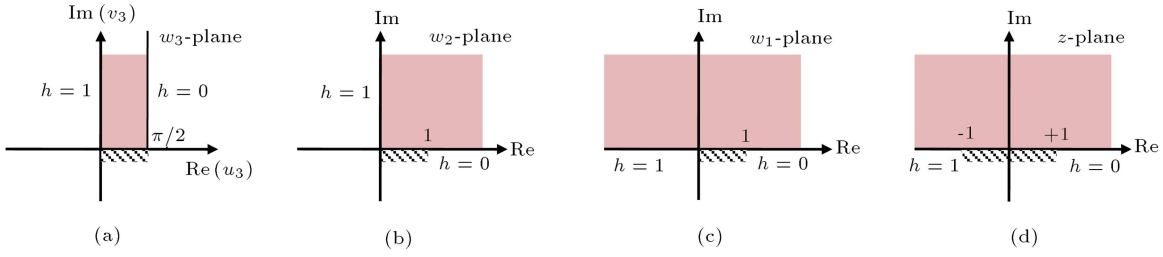

Figure 3. The problem domain under different transformations in complex plane.

$u_k + iv_k$, where k denotes any of the kth planes within which a solution is sought. Therefore, the solution of the problem can be transformed to the upper half-plane in the complex z-plane as follows (see Appendices):

$$\begin{aligned} h(u_3, v_3) &= h(u_3) = h\left(u_3(u_2, v_2)\right) \\ &= h\left(u_3\left(u_2(u_1, v_1), v_2(u_1, v_1)\right)\right) = ... \\ &= h\left(u_3(x, y)\right), \end{aligned} \tag{8}$$

or equivalently:

$$\begin{aligned} h(x, y) =& 1 - \frac{2}{\pi}\sin^{-1}\left(\sqrt{\left(u_2(x, y) + 1\right)^2 + v_2(x, y)^2}\right. \\ & \left. - \sqrt{\left(u_2(x, y) - 1\right)^2 + v_2(x, y)^2}\right). \end{aligned} \tag{9}$$

Finally, the solution in the main problem domain can be found by the following appropriate conformal mapping from the z-plane onto w-plane (Churchill et al. 1974) [44]:

$$w(z) = \frac{H_s}{\pi}\left[\sqrt{(z^2 - 1)} + \cosh^{-1} z\right]. \tag{10}$$

One should notice that this function is a double-valued complex function, owing to the presence of the square root term. To make a proper transform, it is vital to choose a suitable branch cut. To do so, the argument of $z - 1$ can be restricted to $[0, 2\pi]$ and the argument of $z + 1$ can be restricted to $[-\pi, \pi]$. In this way, the function will become a single-valued function along the line segment $[-1, +1]$. These branch cuts are also shown in Figure 2(a) by two dashed lines extended from these two points towards $\pm\infty$.

Note that the solution is obtained for a unit hydraulic head difference between the upstream and the downstream. Since the Laplacian operator is linear (also homogeneous), this normalized solution can be multiplied by H_w to obtain the solution for any actual condition.

As it is necessary to find the gradient of the hydraulic head, ∇h, in the w-plane to calculate the seepage flow force, this can be achieved by making use of the chain rule in partial derivatives of a function which requires the geometrical properties of the transformation of the problem domain from the z-plane onto the w-plane by the Jacobian of the transform:

$$\begin{cases} \frac{\partial w}{\partial x} = \frac{\partial w}{\partial u}\frac{\partial u}{\partial x} + \frac{\partial w}{\partial v}\frac{\partial v}{\partial x} \\ \frac{\partial w}{\partial y} = \frac{\partial w}{\partial u}\frac{\partial u}{\partial y} + \frac{\partial w}{\partial v}\frac{\partial v}{\partial y} \end{cases} \Rightarrow \begin{Bmatrix} \frac{\partial w}{\partial x} \\ \frac{\partial w}{\partial y} \end{Bmatrix} = \begin{bmatrix} \frac{\partial u}{\partial x} & \frac{\partial v}{\partial x} \\ \frac{\partial u}{\partial y} & \frac{\partial v}{\partial y} \end{bmatrix} \begin{Bmatrix} \frac{\partial w}{\partial u} \\ \frac{\partial w}{\partial v} \end{Bmatrix}$$

$$= [J] \begin{Bmatrix} \frac{\partial w}{\partial u} \\ \frac{\partial w}{\partial v} \end{Bmatrix}, \tag{11}$$

or equivalently:

$$\begin{Bmatrix} \frac{\partial w}{\partial u} \\ \frac{\partial w}{\partial v} \end{Bmatrix} = [J]^{-1} \begin{Bmatrix} \frac{\partial w}{\partial x} \\ \frac{\partial w}{\partial y} \end{Bmatrix}, \tag{12}$$

where $[J]$ is the well-known Jacobian matrix. Thus, the seepage flow gradient at every point within the main problem domain in w-plane will be:

$$\begin{aligned} \nabla h &= \frac{\partial h}{\partial u}\mathbf{e_u} + \frac{\partial h}{\partial v}\mathbf{e_v} = \begin{bmatrix} \frac{\partial h}{\partial u} & \frac{\partial h}{\partial v} \end{bmatrix} \begin{bmatrix} \mathbf{e_u} \\ \mathbf{e_v} \end{bmatrix} \\ &= \begin{bmatrix} \frac{\partial h}{\partial u} & \frac{\partial h}{\partial v} \end{bmatrix} [J]^{-T} \begin{bmatrix} \mathbf{e_u} \\ \mathbf{e_v} \end{bmatrix}, \end{aligned} \tag{13}$$

where $\boldsymbol{e_u}$ and $\boldsymbol{e_v}$ are unit base vectors of the complex w-plane with details of equations in Appendix B. Now, the gradient of the flow field, ∇h, can be directly related to the seepage flow force as follows:

$$\mathbf{f_f} = -\mathbf{i}\gamma_w = -\left(\frac{\partial h}{\partial u}\mathbf{e_u} + \frac{\partial h}{\partial v}\mathbf{e_v}\right)\gamma_w, \tag{14}$$

or equivalently in the matrix form:

$$\begin{Bmatrix} f_{fu} \\ f_{fv} \end{Bmatrix} = -\gamma_w \begin{bmatrix} \frac{\partial h}{\partial u} & \frac{\partial h}{\partial v} \end{bmatrix} [J]^{-T} \begin{bmatrix} \mathbf{e_u} \\ \mathbf{e_v} \end{bmatrix}. \tag{15}$$

In these equations, $\mathbf{i}$ is the hydraulic gradient vector, γ_w is the unit weight of the water, and $\boldsymbol{f_f}$ (with components f_{fu} and f_{fv}) is the vector of the unit seepage force, i.e. seepage force per unit volume. The seepage force acts as field of body force with variable magnitude and direction corresponding to the complex nature of the seepage flow pattern through the soil. Figure 4 presents the solution of the flow field for a unit value of H_w/H_s along with the associated hydraulic gradient vector field. In the next part, this vector field is incorporated into equations of the stress field to establish all necessary equations.

4. Solution of the stress field

So far, the solution of the flow force field has been presented. Now, the stress field can be computed throughout the region within which failure would occur. This is done by making use of the well-known method of stress characteristics. The technical literature behind this method and its development date back to Sokolovskii (1960, 1965) [11,46] and later works by a number of authors who employed this method to deal with the bearing capacity or retaining wall problems (Harr, 1966; Houlsby and Wroth, 1982; Bolton and Lau, 1993; Anvar and Ghahramani, 1997; Kumar, 2001; Kumar and Chitikela, 2002; Martin, 2003 and 2005; Veiskarami et al., 2014) [15-17,28,47-51]. We present only the necessary elements of this method as most of

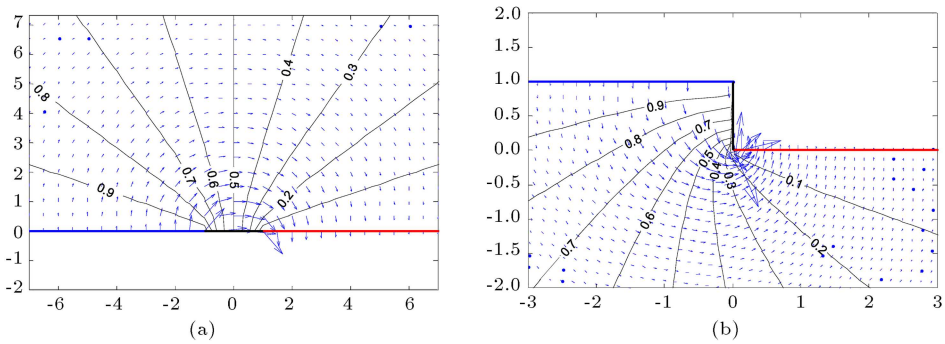

Figure 4. The flow field solution in (a) upper half plane and (b) main problem domain.

the parts can be found in the literature. With notation compatible with traditional ones, a combination of the equilibrium and yield equations yields the necessary stress characteristics equations:

Equilibrium equations:

$$\begin{cases} \frac{\partial \sigma_{xx}}{\partial x} + \frac{\partial \tau_{xy}}{\partial y} = B_x \\ \frac{\partial \sigma_{yy}}{\partial y} + \frac{\partial \tau_{xy}}{\partial x} = B_y \end{cases} \tag{16}$$

Mohr-Coulomb yield criterion:

$$\tau = c + \sigma_n \tan\phi. \tag{17}$$

Components of stress in terms of new variables, σ and θ (according to Kötter, 1903) [52]:

$$\begin{cases} \sigma_{xx} = \sigma(1 + \sin\phi\cos 2\theta) + c\cos\phi\cos 2\theta \\ \sigma_{yy} = \sigma(1 - \sin\phi\cos 2\theta) + c\cos\phi\cos 2\theta \\ \tau_{xy} = \sigma\sin\phi\sin 2\theta + c\cos\phi\sin 2\theta \end{cases} \tag{18}$$

Equations of the stress characteristics directions:

$$\begin{cases} \frac{dy}{dx} = \tan(\theta + \mu) & \text{Positive direction } (\xi) \\ \frac{dy}{dx} = \tan(\theta - \mu) & \text{Negative direction } (\eta) \end{cases} \tag{19}$$

Final forms of the equilibrium-yield equations along the stress characteristics:

$$\begin{cases} d\sigma + 2(\sigma\tan\phi + c)d\theta = \\ \quad -B_x(\tan\phi dy - dx) \\ \quad +B_y(\tan\phi dx + dy) & \text{Along } \xi \\ d\sigma - 2(\sigma\tan\phi + c)d\theta = \\ \quad +B_x(\tan\phi dy + dx) \\ \quad -B_y(\tan\phi dx - dy) & \text{Along } \eta \end{cases} \tag{20}$$

In these equations, σ_{xx}, σ_{yy}, and τ_{xy} are components of the stress tensor at an arbitrary point within the soil mass; B_x and B_y are components of the body force; c and ϕ are soil shear strength parameters defining the Mohr-Coulomb yield criterion; τ and σ_n are components of the shear and normal stress on a failure plane along which the Mohr-Coulomb criterion is satisfied; $\sigma = (\sigma_{xx} + \sigma_{yy})/2$ is the mean stress; θ is the direction of the major principal stress with x-axis and $\mu = \pi/4 - \phi/2$.

One should note that in solution of the stress characteristics equations, the body force includes the submerged unit weight of the soil, γ', as well as the seepage flow force. Assuming that the seepage force encompasses components f_{fx} and f_{fy} along x and y directions, respectively, components of the body force will be:

$$\begin{cases} B_x = -f_{fx} \\ B_y = \gamma' - f_{fy} \end{cases} \tag{21}$$

In addition, the stress measures should be expressed in terms of effective stresses and unit weights in terms of submerged unit weights when the seepage flow is included. The stress field should be then obtained numerically when some appropriate stress boundary conditions are prescribed. With reference to Figure 1(b), there will be two distinct stress boundaries:

Stress boundary along the ground surface, QQ′: In general, the boundary condition along the ground surface (traction free boundary) in presence of a general state of body force, should be defined as follows:

$$\theta_g = \frac{1}{2}\left(\sin^{-1}\left(\frac{\sin\beta}{\sin\phi}\right) - \sin\beta\right), \tag{22}$$

where θ_g is the value of θ along the ground surface and $\tan\beta = B_x/B_y$. In the absence of the lateral component of the body force along the ground surface, $\theta_g = 0$. For more details, one can refer to Kumar (2001), Kumar and Mohan Rao (2002), or Veiskarami and Kumar (2012) [16,30,53].

In addition, σ_g will be:

$$\sigma_g = \frac{1}{2}q_g\left(1 + \tan^2\left(\frac{\pi}{4} + \frac{\phi}{2}\right)\right), \tag{23}$$

where q_g is the surcharge pressure along the ground surface. It is notable that it is convenient to define a very small q_g to prevent trivial solution in the stress characteristics equations. Referring to Bolton and Lau (1993) [48], it is often chosen, such that a dimensionless ratio $= q_g/\gamma' B'$ becomes a very small value, say, less than 0.01.

Stress boundary along the equivalent footing base, BQ: Along this boundary, there is only the value of $\theta = \theta_f$ which should be defined. As stated earlier, it can be assumed that no significant shear stress is mobilized at the equivalent footing interface with the top soil block, APQB, and hence, it is equal to zero.

5. Verifications

Now, the solution strategy obtained so far should be verified. There is no available technique or similar results on the analysis of deep-seated failure in presence of the seepage flow, at least known to the authors. However, a simple and rational procedure was suggested by Terzaghi (1943) [3] for cases without seepage flow which is presented to make preliminary checks. Moreover, this procedure can be extended to the case of the seepage flow by artificial techniques based on simplified assumptions. As an example problem, an arbitrary case of a supported vertical cut into a layer of uniform sand with and without seepage flow is analyzed. Since all dimensions are normalized to the height of the cut, H_s, thus, it is automatically equal to 1. Soil characteristic parameters are $\gamma' = 10$ kN/m^3 and $\phi' = 25°$. Analyses were made by using Eq. (1) for the factor of safety.

Results of the analyses are presented in Table 1. In Case 1, the hydraulic head difference, H_w, between the upstream and downstream water levels is zero. In other cases, this difference grows to a critical value. In addition, when applying the method of Terzaghi (1943) [3] to cases with seepage flow, it is conservatively assumed that the hydraulic head is linearly dissipated along the wall length. Therefore, a very rough and conservative estimate of the hydraulic gradient has been made. The hydraulic gradient obtained by this way is reasonably higher than the average hydraulic gradient within the soil block which is simply $i_d = H_w/H_s$. This hydraulic gradient is then used to amplify the weight of the soil block to be supported by the equivalent footing. Instead, no correction is accounted for the seepage flow through the plastic region beneath the equivalent footing and conventional bearing capacity factor, N_γ, implemented. In addition, Terzaghi (1943) [3], based on numerical results for cases without inclusion of the seepage flow, showed that the width of the equivalent footing, i.e., the B'/H_s ratio, falls within the range of 0.18 to 0.19. For those cases analyzed by Terzaghi's method, this ratio is assumed to be 0.19.

In application of Eq. (1) when using Terzaghi (1943) method, the third bearing capacity factor, N_γ, was taken as 9.7 [3]. In addition, another try was made based on the numerical results of N_γ by Bolton and Lau (1993) [48] by the method of stress characteristics which gave $N_\gamma = 3.51$. The downward seepage flow force (to be added to the weight of the soil block), F_{fd}, was equal to 0.19 $i_d H_s^2$. Also, the shear resistance, S, mobilized along the soil block was assumed to be:

$$S = \frac{1}{2}\gamma' H_s^2 K_A \tan\phi', \tag{24}$$

where K_A is the active earth pressure coefficient. This latter assumption on S was also chosen as suggested by Terzaghi (1943) [3].

In the present approach, however, neither of the abovementioned assumptions is made. A more precise calculation based on the present procedure can be performed where the average of the hydraulic gradient through the soil block can be calculated. Moreover, the bearing capacity of the equivalent footing has been

Table 1. Results of the stability analysis for example problem.

Method	Case 1: $H_w/H_s = 0$ (no flow)		Case 2: $H_w/H_s = 0.25$		Case 3: $H_w/H_s = 0.50$	
	B'_{cr}	$F_s^{\min}$	B'_{cr}	$F_s^{\min}$	B'_{cr}	$F_s^{\min}$
Conventional approach (Terzaghi, 1943)	0.19	3.699	0.19	3.466	0.19	3.283
Conventional approach (Bolton and Lau, 1993)	0.19	1.329	0.19	1.254	0.19	1.188
Present study[1]	0.19	1.267	0.27	1.079	0.31	0.941
Present study[2]	0.19	1.267	0.26	1.243	0.29	1.040

[1] Variable seepage force; [2] Constant seepage force (averaged value).

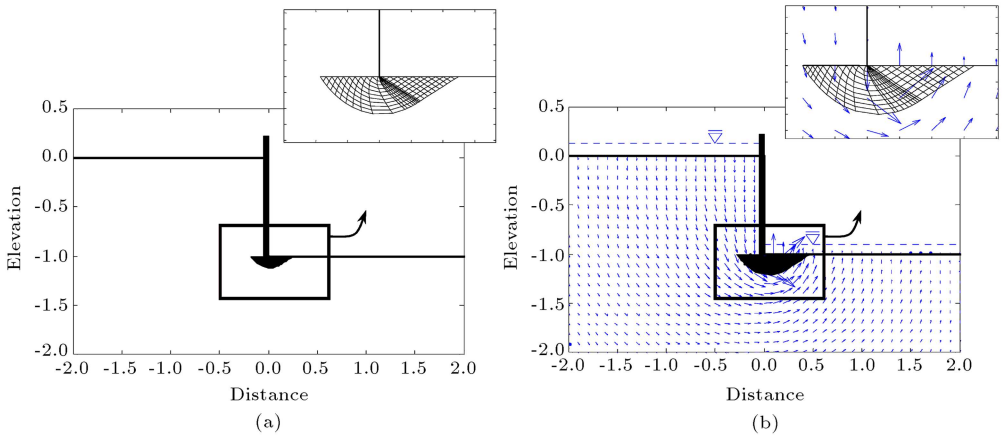

Figure 5. Solution of the stress field: (a) Without seepage flow ($H_w = 0$) and (b) with seepage flow ($H_w/H_s = 0.25$).

calculated with inclusion of the seepage flow effects. It is notable that the critical width of the equivalent footing, B'_{cr}, has been obtained corresponding to the least factor of safety, $F_s^{\min}$. Figure 5 shows the solution of the stress field (failure pattern) for two cases in the absence and in presence of the seepage flow with the zone of failure being enlarged. It is obvious that the size of the plastic region grows when the intensity of the seepage flow increases. This is logical as a larger passive zone is required to withstand the unbalancing force at the limiting equilibrium with increasing seepage force.

Another important point in computation of the stress field in the present approach is that the flow force is a non-uniform vector field. The variation in the direction and magnitude of the flow force from point to point renders the required numerical computations for the stress field difficult and much more mesh refinements may be required to get a rational result. To avoid this disadvantage, another simplified approach is suggested, that is, to use the averaged values of the flow force, as an equivalent constant flow field within the entire plastic region. To do so, an iteration approach can be made to calculate the flow force at every nodes of the stress characteristics network and to take an average value for the next round of iteration. It was done, and fortunately two interesting results were observed. First, the convergence was achieved very quickly (in most cases, a total number of 5 to 10 iterations make the results stable). Second, the difference between the variable flow field and the equivalent constant flow field is not practically significant. Table 1 presents the results of both approaches for the example problem outlined before. The first approach, i.e. the variable flow field is denoted by a superscript 1; the second approach, i.e. using an equivalent constant flow field, is denoted by a superscript 2. The difference is about 10% which is practically negligible and makes the simplified approach a more efficient alternative.

It is important to note that the convergence criterion in the simplified approach has been checked by not only the stability of the solution for the factor of safety, but also for other different factors. In essence, the convergence was checked by convergence of the stress field at each computational step, i.e. through the stepwise solution of the stress field as well as the convergence of the geometry of stress characteristics network. Therefore, the convergence criterion was achieved when the extent of the plastic region as well as the stress field was computed. The last criterion was the convergence of the factor of safety.

6. Stability charts

In this section, a number of analyses were made to present the results in a more practical manner. With reference to Figure 6, which reflects the results of these analyses, two different charts were developed. One of them is the variation of the least factor of safety, F_s, with H_w/H_s for a certain soil friction angle. The other is the critical value of the relative dimension of the equivalent footing size, B'/H_s, i.e. the one with the lowermost factor of safety. In all these analyses, the soil submerged unit weight as well as the unit weight of the water were assumed to be 10 kN/m^3 which seems to be practically reasonable. In addition, the minimum factor of safety was obtained by an iterative analysis to find the equivalent footing size for which the factor of safety becomes a minimum.

In the first plot shown in Figure 6(a), variations of the safety factor, F_s, is plotted against the nondimensional ratio, H_w/H_s, for a range of friction angles between 20° and 40°. It is evident that for higher friction angles, the factor of safety is very high, and hence, there is no significant risk of deep seated failure. In contrast, in lower friction angles, the deep-seated failure is prone to occur, even in the absence of the seepage flow. For example, the factor of safety is always below 1 when $\phi' = 20°$ and less, which means the deep-seated failure is always a major concern. When the friction angle ranges between 20° and 30°, the deep-

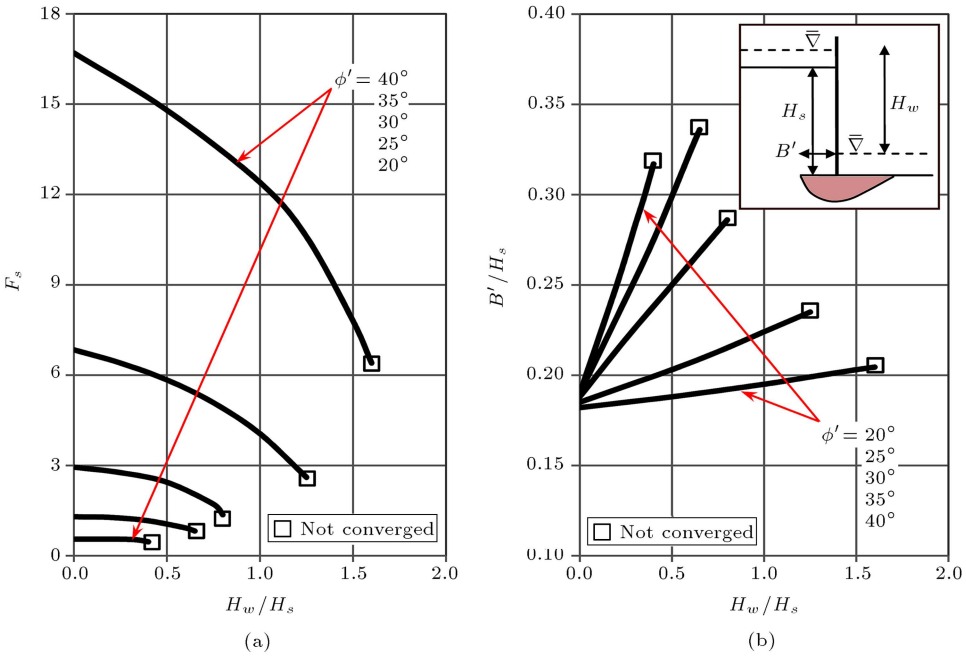

Figure 6. Variations of the factor of safety (a) and the critical value of the equivalent footing width (b) versus H_w/H_s.

seated failure may or may not be critical, depending on the H_w/H_s ratio. It is worth noting that the last points of these charts mark the point beyond which the numerical analyses became unstable and no rational solution could be found, since such a numerical instability seems to have a physical meaning, e.g. local instability in a portion of the soil mass in terms of "static liquefaction" (even for $F_s > 1$); therefore, the last points of these charts could be regarded as a critical limit for the H_w/H_s. Beyond these points, the factor of safety drops very quickly as H_w/H_s increases. Therefore, it seems that no extrapolation of these charts is admissible.

In the second plot shown in Figure 6(b), variations of the equivalent footing width, B'/H_s, are shown versus H_w/H_s for a practical range of friction angles between 20° and 40°. According to Terzaghi (1943) [3], this ratio often ranges between 0.18 and 0.19 for common range of the soil friction angle when there is no seepage flow. However, an insight into the results indicates that the equivalent footing size increases as the non-dimensional ratio, H_w/H_s, increases. This can be interpreted in accordance with the nonlinear nature of the equation for the factor of safety. This equation depends on both the body forces (which have their magnitude and direction changed throughout the problem domain) and the equivalent footing width in a nonlinear fashion; hence, its extrema change with changing H_w/H_s and friction angle. However, in spite of its mathematical meaning, its physical meaning will be of greater importance. It is clear from the figures that as the soil friction angle becomes smaller, the size of the equivalent footing becomes larger. This indicates that if a deep-seated failure occurs, the size of the failure zone becomes larger with certainly more catastrophic effects. Therefore, not only is the factor of safety against deep-seated failure lower in soils possessing lower friction angles, but also the zone of influence of the collapse is larger.

In addition, a rule of thumb indicates that when the ratio H_w/H_s reaches around unity, the soil may experience the critical hydraulic gradient at the edge of the cut. Although this fact may initiate a local progressive failure, the edge of the cut is a singular point where neither the stress nor the flow field cannot be properly computed. Therefore, the computational procedure can advance until the hydraulic gradient reaches some critical value within the plastic region (not at the singular point).

With reference to the presented charts, another important note should be pointed, i.e. the numerical solution to the stress field cannot be achieved when the hydraulic gradient exceeds some critical value (even at just one point within the field). Beyond this critical value, the solution will not converge. Note that this can be regarded as a disadvantage to the procedure outlined here. In fact, if only one point does not converge, the computational efforts cannot be completed, although this might be just a local failure without necessarily a total loss of strength in the entire soil mass. The critical value of the hydraulic gradient in a horizontal seepage flow with regard to the Coulomb failure criterion can be found as $i_{cr}\,\gamma_w/\gamma' = \tan\phi'$ [30]. However, in a complex form of the seepage flow, it cannot be easily computed unless numerically. Therefore, it is not surprising that the graphs representing variations of F_s with

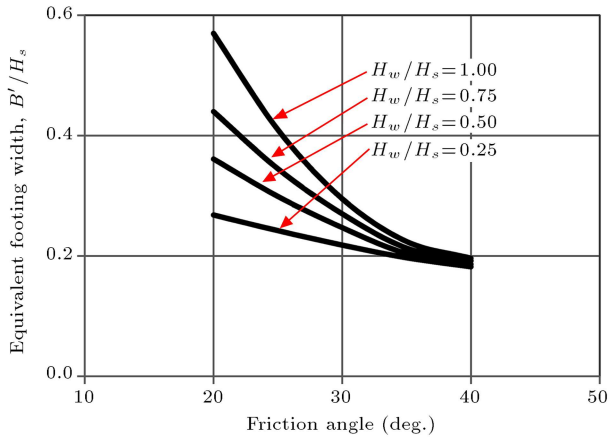

Figure 7. Variations of the equivalent footing width, B'/H_s with ϕ'.

H_w/H_s are terminated at some point different from $F_s = 0$. These points are denoted by a small square (i.e., was not converged) in the presented graphs. In addition, these points have a physical meaning, i.e. when the soil becomes unstable at some point within the plastic region, this instability becomes the onset of a progressive failure starting just from that particular point. Furthermore, as soon as this instability is reached, the initiation of a failure should be expected in spite of the overall factor of safety (which may be still higher than unity). Thus, it is not sufficient to have a factor of safety higher than unity, but it is necessary to avoid approaching such critical points following a progressive failure.

Finally, variations of the equivalent footing width, B'/H_s, with the soil friction angle are plotted in Figure 7. One should note that a small part of these graphs has been produced back by extrapolation of the results (for $\phi' = 20°$ and 25° only). Such curves could not be produced with sufficient accuracy for friction angle ϕ' below 20° due to convergence error. These plots are useful for a simplified approach based on an average of the hydraulic gradient.

7. Conclusions

A semi-analytical study was performed to include the effect of the seepage flow on the stability of a supported vertical cut against deep-seated (or base) failure in waterfront excavations. This is a problem for which no analytical solution is available and numerical techniques involve complications. In the presented semi-analytic procedure, the effect of the seepage flow has been included by solution of the flow field as an independent and analytical solution (background solution) and the solution of the stress field at the limiting equilibrium as the main solution (by numerical techniques). In this procedure, it is formally assumed that the flow field pattern is not influenced by the formation of a failure mechanism. Such an assumption does not seem to be too much restrictive; hence, the solution of the flow field can be found independently. The solution of the flow field was found by successive applications of conformal mappings in complex planes and the simple solution of the steady-state flow problem in a semi-infinite strip in the complex plane. The presented approach has several advantages over other fully numerical methods, e.g. higher accuracy and speed.

Analyses showed that the deep-seated failure is often a critical criterion to design supported excavations, which deserves more attention. In fact, for practical range of friction angle for most sands, the probability of failure increases significantly when the cut is exposed to the seepage flow. In cases with low friction angle, like fine sands, such a failure may dominate the design and may precede other types of failure such as the slope failure (often not a major concern), wall failure (due to insufficient passive pressure and increased active pressure) or piping, and heaving failures. In addition, results revealed that the size of the collapse pattern grows significantly as the soil friction angle decreases. Thus, it can be concluded that not only the probability of failure can increase for such soils, but also the type of failure can be more catastrophic which requires further serious provisions in practice.

References

1. Coulomb, C. A., *Essay on an Application of the Rules of Maximal and Minimal to Some Problems of Statics Relating to Architecture*, [Essai sur une Application des Règles des Maximisn et Minimis á QuelquesProblèmes de Statique Relatifs á L'Architecture], 7. Paris, France: Mem. Acad. Roy. Pres. Div. Sav. (1776).
2. Rankine, W.J.M., *On the Stability of Loose Earth. London*, UK: Phil. Trans. Royal Soc. (1857).
3. Terzaghi, K., *Theoretical Soil Mechanics*, NY: John-Wiley and Sons Inc.(1943).
4. Kumar, J. and Subba Rao, K.S. "Passive pressure coefficients, critical failure surface and its kinematic admissibility", *Götechnique*, **47**(1), pp. 185-192 (1997).
5. Subba Rao, K.S. and Choudhury, D. "Seismic passive earth pressures in soils", *Journal of Geotechnical and Geoenvironmental Engineering, ASCE*, **131**(1), pp. 131-135 (2005).
6. Barros, P.L.A. "A coulomb-type solution for active earth thrust with seepage", *Göotechnique*, **56**(3), pp. 159-164 (2006).
7. Ghosh, P. "Seismic active earth pressure behind a non-vertical retaining wall using pseudo-dynamic analysis", *Can. Geotech. J.*, **45**(1), pp. 117-123 (2008).
8. Ghosh, S. and Sharma, R.P. "Pseudo-dynamic evaluation of passive response on the back of a retaining wall

supporting c-φ backfill", *Geomechanics and Geoengineering: An International Journal*, Taylor and Francis, **7**(2), pp. 115-121 (2012).

9. Barros, P.L.A. and Santos, P.J. "Coefficients of active earth pressure with seepage effect", *Can. Geotech J.*, **49**(6), pp. 651-658 (2012).
10. Ling, H., Ling, H.I. and Kawataba, T. "Revisiting nigawa landslide of the 1995 Kobe earthquake", *Göotechnique*, **64**(5), pp. 400-404 (2014). DOI: 10.1680/geot.12.T.019
11. Sokolovskii, V.V., *Statics of Granular Media*, London: Pergamon (1965).
12. Larkin, L.A. "Theoretical bearing capacity of very shallow footings", *Journal of the Soil Mechanics and Foundations Division ASCE*, **94**(6), pp. 1347-1357 (1968).
13. Sabzevari, A. and Ghahramani, A. "The limit equilibrium analysis of bearing capacity and earth pressure problems in nonhomogeneous soils", *Soils and Foundations, Japanese Society of Soil Mechanics and Foundations Engineering*, **12**(3), pp. 33-48 (1972).
14. Sabzevari, A. and Ghahramani, A. "Theoretical investigation on the passive progressive failure in an earth pressure problem", *Soils and Foundations, Japanese Society of Soil Mechanics and Foundations Engineering*, **13**(2), pp. 1-18 (1973) .
15. Houlsby, G.T. and Wroth, C.P. "Direct solution of plasticity problems in soils by the method of characteristics", *Proc. 4th Intl. Conf. Num. Meth. Geomech., Edmonton*, **3**, pp. 1059-1071 (1982).
16. Kumar, J. "Seismic passive earth pressure coefficients for sands", *Can. Geotech. J.*, **38**(4), pp. 876-881 (2001).
17. Kumar, J. and Chitikela, S. "Seismic passive earth pressure coefficients using the method of characteristics", *Can. Geotech. J.*, **39**(2), pp. 463-471 (2002).
18. Chen, W.-F. "Soil mechanics and theorems of limit analysis", *Journal of the Soil Mechanics and Foundations Division, ASCE*, **95**(SM2), pp. 493-518 (1969).
19. Lysmer, J. "Limit analysis of plane problems in soil mechanics", *Journal of the Soil Mechanics and Foundations Division, ASCE*, **96**(SM4), pp. 1311-1334 (1970).
20. Chen, W-F. and Davidson, H.L. "Bearing capacity determination by limit analysis", *Journal of the Soil Mechanics and Foundations Division, ASCE*, **99**(SM6), pp. 433-449 (1973).
21. Collins, I.F. "A note on the interpretation of coulomb's analysis of the thrust on a rough retaining Wall in terms of the limit theorems of plasticity theory", *Göotechnique*, **23**(3), pp. 442-447(1973).
22. Chen, W-F., *Limit Analysis and Soil Plasticity*, Elsevier (1975).
23. Arai, K. and Jinki, R. "A lower-bound approach to active and passive earth pressure problems", *Soils and Foundations. Japanese Society of Soil Mechanics and Foundations Engineering*, **30**(4), pp. 25-41 (1990) .
24. Soubra, A.-H. "Static and seismic passive earth pressure coefficients on rigid retaining structures", *Can. Geotech. J.*, **37**(1), pp. 463-478 (2000).
25. Soubra, A-H. and Macuh, B. "Active and passive earth pressure coefficients by a kinematical approach", *Geotechnical Engineering*, **155**(2), pp. 119-131 (2002).
26. Shiau, J.S., Augarde, C.E., Lyamin, A.V. and Sloan, S.W. "Finite element limit analysis of passive earth resistance in coehesionless soils", *Soils and Foundations*, **48**(6), pp. 843-850 (2008).
27. Jahanandish, M., Veiskarami, M. and Ghahramani, A. "Effect of stress Level on the bearing capacity factor, N_γ, by ZEL Method", *KSCE Journal of Civil Engineering*, Springer, **14**(5), pp. 709-723 (2010).
28. Veiskarami, M., Kumar, J. and Valikhah, F. "Effect of the flow rule on the bearing capacity of strip foundations on sand by the upper-bound Limit analysis and slip lines", *International Journal of Geomechanics, ASCE*, **14**(3), 04014008 (2014). DOI: 10.1061/(ASCE)GM.1943-5622.0000324
29. Kawamura, M. and Watanabe, T. "Stress analysis of earth pressure with seepage flow during heavy rainstorms", *Proc. 9th Southeast Asian Geotechnical Conference*, Publication in Bangkok: Southeast Asian Geotechnical Society. Bangkok, 7-11 Dec. 1987 (1) 2.53-2.62, (1989). DOI: 10.1016/0148-9062(89)92828-3
30. Kumar, J. and Chakraborty, D. "Bearing capacity of foundations with inclined ground water seepage", *International Journal of Geomechanics, ASCE*, **13**(5), pp. 611-624 (2013).
31. Veiskarami, M. and Kumar, J. "Bearing capacity of foundations subjected to groundwater flow", *Geomechanics and Geoengineering: An International Journal, Taylor and Francis*, **7**(4), pp. 293-301 (2012).
32. Soubra, A.-H., Kastner, R. and Benmansour, A. "Passive earth pressures in the presence of hydraulic gradients", *Göotechnique*, **49**(3), pp. 319-331 (1999).
33. Benmebarek, N., Benmebarek, S., Kastner, R. and Soubra, A.-H. "Passive and active earth pressures in the presence of groundwater flow", *Göotechnique*, **56**(3), pp. 149-158 (2006).
34. Santos, P.J. and Barros, P.L.A. "Active earth pressure due to a soil mass partially subjected to water seepage", *Can. Geotech. J.*, (In Press) (2015). DOI: 10.1139/cgj-2014-0367)
35. Veiskarami, M. and Zanj, A. "Stability of sheet-pile walls subjected to seepage flow by slip lines and finite elements", *Göotechnique*, **64**(10), pp. 759-775 (2014).
36. Craig, R.F., *Soil Mechanics*, 4th Ed., Chapman and Hall, London, UK (1987).
37. Bowles, J.E., *Foundation Analysis and Design*, 5thEd., McGraw Hill, New York, USA (1996).

38. Veiskarami, M. and Habibagahi, G. "Foundations bearing capacity subjected to seepage by the kinematic approach of the limit analysis", *Frontiers of Structural and Civil Engineering*, **7**(4), pp. 446-455 (2013).
39. Harr, M.E., *Groundwater and Seepage*, McGraw-Hill, New York (1962).
40. Christian, J.T. "Flow nets from finite-element data", *Int. J. Numer. Anal. Meth. Geomech.*, John-Wiley and Sons, **4**(2), pp. 191-196 (1980).
41. Griffiths, D.V. "Seepage beneath unsymmetric cofferdams", *Göotechnique*, **44**(2), pp. 297-305 (1994).
42. Zienkiewicz, O.C. and Taylor, R.L., *The Finite Element Method*, 5th Ed. Butterworth-Heinemann, UK (2000).
43. Kiousis, P.D. "Least-squares finite-element evaluation of flow nets", *Journal of Geotechnical and Geoenvironmental Engineering, ASCE*, **128**(8), pp. 699-701 (2002).
44. Churchill, R.V., Brown, J.W. and Verhey, R.F., *Complex Variables and Applications*, 3rd Ed., McGraw Hill, New York, USA (1974).
45. Mathews, J.H. and Howell, R.W., *Complex Analysis for Mathematics and Engineering*, 3rd Ed., Jones and Bartlett, Sudbury, Massachusetts, USA (1997).
46. Sokolovskii, V.V., *Statics of Soil Media* (translated by D.H. Jones and A.N. Schofield)., Butterworths, London, UK (1960).
47. Harr, M.E., *Foundations of Theoretical Soil Mechanics*, McGraw-Hill, NY, USA (1966).
48. Bolton, M.D. and Lau, C.K. "Vertical bearing capacity factors for circular and strip footings on Mohr-Coulomb soil", *Can. Geotech. J.*, **30**(6), pp. 1024-1033 (1993). DOI: 10.1139/t93-099.
49. Anvar, S.A. and Ghahramani, A. "Equilibrium equations on zero extension lines and their application to soil engineering", *Iranian Journal of Science and Technology (IJST)*, Shiraz University Press, Transaction B, **21**(1), pp. 11-34 (1997).
50. Martin, C. M. "ABC - analysis of bearing capacity (user guide for)" OUEL Report No. 2261/03, University of Oxford, UK, (2003). URL: http://www.eng.ox.ac.uk/civil/people/cmm/software
51. Martin, C.M. "Exact bearing capacity calculations using the method of characteristics", *Proc. 11th Int. Conf. ofIACMAG*, **4**, Turin, France, pp. 441-450 (2005).
52. Kötter, F., *Determination of Pressure on Curved Sliding Surfaces, a Task from the Theory of Earth Pressure* [Die Bestimmung des Druckes an gekrümmten Gleitflächen, eine Aufgabe aus der Lehre vom Erddruck], Sitzungsberichte der Akademie der Wissenschaften, pp. 229-233, Berlin, Germany (1903).
53. Kumar, J. and Mohan-Rao. "Seismic bearing capacity factors for spread foundations", *Göotechnique*, **52**(2), pp. 79-88 (2002).

Appendix A

Successive transformations from w_3-plane to z-plane

The problem domain and the solution can be transformed from w_3-plane to z-plane by the following successive conformal mappings. With reference to Figure 3:

$$w_3 = \sin^{-1} w_2 \text{ or inversely: } w_= \sin w_3. \tag{A.1a}$$

Moreover:

$$w_2 = u_2 + iv_2 = \sin(u_3 + iv_3) = \sin u_3 \cosh v_3 + i \cos u_3 \sinh v_3. \tag{A.1b}$$

Therefore:

$$u_2 = \sin u_3 \cosh v_3 \text{ and } v_2 = \cos u_3 \sinh v_3. \tag{A.1c}$$

However, according to trigonometric relationships:

$$\left(\frac{u_2}{\sin u_3}\right)^2 - \left(\frac{v_2}{\cos u_3}\right)^2 = 1. \tag{A.1d}$$

Thus:

$$u_3 = \sin^{-1}\left(\sqrt{(u_2+1)^2+v_2^2} - \sqrt{(u_2-1)^2+v_2^2}\right), \tag{A.1e}$$

which is required for the rest of calculations.

Transformation between w_1-plane and w_2-plane is obtained by:

$$w_2 = w_1^{1/2} \text{ or inversely } w_1 = w_2^2. \tag{A.2a}$$

Consequently:

$$u_1 + iv_1 = (u_2 + iv_2)^2. \tag{A.2b}$$

which yields:

$$\begin{cases} u_2 = \pm\frac{1}{\sqrt{2}}\sqrt{u_1 \pm \sqrt{u_1^2+v_1^2}} \\ v_2 = \frac{v_1}{2u_2} = \frac{v_1}{2u_2} \end{cases} \tag{A.2c}$$

Transformation between z-plane and w_1-plane is obtained by:

$$w_1 = \frac{z+1}{2} \text{ or inversely: } z = 2w_1 - 1. \tag{A.3a}$$

Therefore:

$$u_1 = \frac{x+1}{2} \text{ and } v_1 = \frac{y}{2}. \tag{A.3b}$$

These transformations can be directly used to transfer both the geometry and the solution of the problem; hence, the solution will be available in complex z-plane.

Appendix B

Solution of the hydraulic gradient in complex w-plane

The gradient of the hydraulic head required to compute the seepage flow force can be found as follows.

First of all, one should obtain the Jacobian of the transformation which requires some artificial manipulations by the aid of functions $\mathrm{Re}(w(z))$ and $\mathrm{Im}(w(z))$ which bring the real and imaginary parts of a complex function and can be easily programmed in MATLAB or other similar environments:

$$[J] = \begin{bmatrix} \frac{\partial u}{\partial x} & \frac{\partial v}{\partial x} \\ \frac{\partial u}{\partial y} & \frac{\partial v}{\partial y} \end{bmatrix}, \tag{B.1}$$

$$\frac{\partial u}{\partial x} = -\frac{1}{\pi}\mathrm{Re}\left(\frac{2x+2iy}{2\sqrt{(x+iy)^2-1}} + \frac{1}{\sqrt{(x+iy)^2-1}}\right), \tag{B.2}$$

$$\frac{\partial u}{\partial y} = -\frac{1}{\pi}\mathrm{Re}\left(\frac{2ix-2y}{2\sqrt{(x+iy)^2-1}} + \frac{i}{\sqrt{(x+iy)^2-1}}\right), \tag{B.3}$$

$$\frac{\partial v}{\partial x} = -\frac{1}{\pi}\mathrm{Im}\left(\frac{2x+2iy}{2\sqrt{(x+iy)^2-1}} + \frac{1}{\sqrt{(x+iy)^2-1}}\right), \tag{B.4}$$

$$\frac{\partial v}{\partial y} = -\frac{1}{\pi}\mathrm{Im}\left(\frac{2ix-2y}{2\sqrt{(x+iy)^2-1}} + \frac{i}{\sqrt{(x+iy)^2-1}}\right). \tag{B.5}$$

Having known the coordinates of an arbitrary point, in the main problem domain, the inverse of the Jacobian matrix can be found for the rest of calculations. In addition, the components of the gradient of the hydraulic head, $\boldsymbol{\nabla} h$, can be calculated by Eqs. (B.6) to (B.8) as shown in Box I.

It is notable that the inverse problem, i.e. mapping from the w-plane onto the z-plane, may be a little complicated and long; however, the location of every arbitrary point in the w-plane can be found by a numerical technique like the Newton-Raphson method as the entire problem, i.e. solution of the flow field and later, solution of the stress field, should be traditionally recast in a computer code.

Biographies

Mehdi Veiskarami has received his BSc and MSc degrees from the University of Guilan and received his PhD degree from Shiraz University in 2010 under supervision of Prof. Arsalan Ghahramani and Prof. Mojtaba Jahanandish. His PhD dissertation was on the load-displacement behavior and bearing capacity of shallow foundations by the ZEL method, considering the stress level effect. He has published several papers in the field of geomechanics and coauthored a book on mat foundations analysis and design which was published by the University of Guilan press in 2006. Dr. Mehdi Veiskarami is currently serving as a faculty member and visiting scholar at Shiraz University while he is simultaneously an Assistant Professor in the University of Guilan.

Sina Fadaie has received both BSc and MSc degrees from the University of Guilan. During his master program, he was awarded the outstanding graduate student and his thesis was recognized as one of the selected theses in the area of Geotechnical Engineering in Guilan Province by a research council determined by the municipality of Rasht. His master thesis was on the stability of supported vertical cuts against deep-seated failure when they are prone to the seepage flow by a hybrid numerical method. He worked under supervision of Dr. Mehdi Veiskarami in the University of Guilan and graduated in early 2016. He has recently published several papers from his research results.

$$\boldsymbol{\nabla} h = \frac{\partial h}{\partial x}\mathbf{e_x} + \frac{\partial h}{\partial y}\mathbf{e_y}, \tag{B.6}$$

$$\frac{\partial h}{\partial x} = -\frac{1}{\pi}\left(\frac{-\frac{x-1}{2\sqrt{(x-1)^2+y^2}} + \frac{x+1}{2\sqrt{(x+1)^2+y^2}}}{\left(\sqrt{(x+1)^2+y^2}\right) / \left(1 - \frac{1}{2}\sqrt{(x-1)^2+y^2} - \frac{1}{2}\sqrt{(x+1)^2+y^2}\right)^2}\right)^{\frac{1}{2}}, \tag{B.7}$$

$$\frac{\partial h}{\partial y} = -\frac{1}{\pi}\left(\frac{-\frac{y}{2\sqrt{(x-1)^2+y^2}} + \frac{x+1}{2\sqrt{(x+1)^2+y^2}}}{\left(1 - \frac{1}{2}\sqrt{(x-1)^2+y^2} - \frac{1}{2}\sqrt{(x+1)^2+y^2}\right)^2}\right)^{\frac{1}{2}}. \tag{B.8}$$

Box I